Dig Dis Sci (2012) 57:2580–2591
DOI 10.1007/s10620-012-2217-1

ORIGINAL ARTICLE

Soluble Epoxide Hydrolase Gene Deficiency or Inhibition Attenuates Chronic Active Inflammatory Bowel Disease in IL-10(−/−) Mice

Wanying Zhang · Allison L. Yang · Jie Liao · Haonan Li · Hua Dong · Yeon Tae Chung · Han Bai · Kristina A. Matkowskyj · Bruce D. Hammock · Guang-Yu Yang

Received: 1 November 2011 / Accepted: 25 April 2012 / Published online: 16 May 2012

Abstract
Background Soluble epoxide hydrolase (sEH) metabolizes anti-inflammatory epoxyeicosatrienoic acids (EETs) into their much less active dihydroxy derivatives dihydroxyeicosatrienoic acids. Thus, targeting sEH would be important for inflammation.
Aims To determine whether knockout or inhibition of sEH would attenuate the development of inflammatory bowel disease (IBD) in a mouse model of IBD in IL-10(−/−) mice.
Methods Either the small molecule sEH inhibitor *trans*/-4-[4-(3-adamantan-1-yl-ureido)-cyclohexyloxy]-benzoic acid (*t*-AUCB) or sEH knockout mice were used in combination with IL-10(−/−) mice. *t*-AUCB was administered to mice in drinking fluid. Extensive histopathologic, immunochemical, and biochemical analyses were performed to evaluate effect of sEH inhibition or deficiency on chronic active inflammation and related mechanism in the bowel.
Results Compared to IL-10 (−/−) mice, sEH inhibition or sEH deficiency in IL-10(−/−) mice resulted in significantly lower incidence of active ulcer formation and transmural inflammation, along with a significant decrease in myeloperoxidase-labeled neutrophil infiltration in the inflamed bowel. The levels of IFN-γ, TNF-α, and MCP-1, as well VCAM-1 and NF-kB/IKK-α signals were significantly decreased as compared to control animals. Moreover, an eicosanoid profile analysis revealed a significant increase in the ratio of EETs/DHET and EpOME/DiOME, and a slightly down-regulation of inflammatory mediators LTB_4 and 5-HETE.
Conclusion These results indicate that sEH gene deficiency or inhibition reduces inflammatory activities in the IL-10 (−/−) mouse model of IBD, and that sEH inhibitor could be a highly potential in the treatment of IBD.

Keywords Inflammatory bowel disease · Soluble epoxide hydrolase · Ephx2 gene · IL-10 deficient mice · Oxylipin profile

Introduction

Soluble epoxide hydrolase (sEH) is a pro-inflammatory enzyme involving in metabolism of the epoxygenated products of arachidonic acid, including epoxyeicosatetraenoic acid (EETs) [1]. Physiologic concentrations of EETs inhibit inflammation by decreasing cytokine-induced endothelial cell adhesion molecule expression and inhibiting NF-κB and I$\kappa\kappa$ kinase [2]. Pharmacological inhibition of sEH such as *trans*/-4-[4-(3-adamantan-1-yl-ureido)-cyclohexyloxy]-benzoic acid (*t*-AUCB) has shown to increase plasma EET concentrations and has demonstrated a potent anti-inflammatory activity [1, 3–11], in the models

Wanying Zhang and Allison L. Yang contributed equally to this work.

Electronic supplementary material The online version of this article (doi:10.1007/s10620-012-2217-1) contains supplementary material, which is available to authorized users.

W. Zhang · A. L. Yang · J. Liao · H. Li · Y. T. Chung · H. Bai · K. A. Matkowskyj · G.-Y. Yang (✉)
Department of Pathology, Feinberg School of Medicine, Northwestern University, 303 East Chicago Avenue, Chicago, IL 60611, USA
e-mail: g-yang@northwestern.edu

H. Dong · B. D. Hammock
Department of Entomology, University of California, One Shields Avenue, Davis, CA 95616, USA

including LPS-induced systematic inflammation in mice, tobacco–induced bronchitis, cardiac hypertrophy, and renal inflammation [6, 12]. Thus, it is attractive to speculate that inhibition of sEH may be beneficial as a novel therapeutic option in reducing inflammatory processes in chronic active inflammatory bowel disease (IBD).

IBD, including ulcerative colitis (UC) and Crohn's disease (CD), is a longstanding chronic inflammation in the bowel with unknown etiology [13]. The prevalence of these chronic inflammatory diseases has shown an upward trend and the incidence per year ranges from 5 to 18 cases per 100,000 [14, 15]. Current strategies for the treatment of IBD are aimed at reducing activity of inflammation, and commonly used medications are 5-aminosalicylate (5-ASA). However, these compounds are only clinically useful for mild to moderate active IBD and are more useful in UC than in Crohn's disease [16]. Thus, it is crucial to develop a more efficient anti-inflammatory agent to combat inflammation.

There have been multiple animal models of IBD. The genetically-engineered and chemically-induced mouse models, used in combination with pharmacological agents, and active anti-inflammatory food components, have proven to be especially useful in the study of the mechanisms, prevention, and treatment of IBD. Herein, there are two particular genes of interest when using genetically-engineered mouse models as a direct experimental approach: IL-10 and sEH. IL-10 is an important regulatory anti-inflammatory cytokine and has been associated with the development of IBD when it is defective [17]. In IL-10 knock-out mouse models, 100 % of the mice will develop inflammation in the duodenum, proximal jejunum, and proximal colon; but occurrence of IBD greatly varies from 3 to 12 months which can be overcome through the short-period administration of piroxicam to synchronize the development of IBD [18]. Histopathology shows active ulcer formation and transmural inflammation that highly mimics Crohn's disease in IL-10 knock-out mice. Conversely, sEH knock-out mice are phenotypically normal with only minimally decreased body weight in males, but have an altered arachidonic acid metabolism [19]. Previous studies have shown that sEH knockout in mice (disruption of Epx2 gene which encodes sEH) results in a significant shift of the epoxy-fatty acid to diol ratio, further led to protect against myocardial ischemia–reperfusion injury, modulate the inflammatory response to cerebral ischemia, and improve glucose homeostasis [20–22].

In the present study, we determined whether the inhibition or knock-out of sEH affected the development and progression of IBD in IL-10(−/−) mice. The development of chronic active IBD was histopathologically and immunochemically analyzed in sEH and IL-10 double knock-out mice [sEH(−/−)/IL-10(−/−)] and IL-10(−/−) mice treated with sEH inhibitor *t*-AUCB as compared to IL-10 (−/−), sEH (−/−), and wild-type mice. The effect of sEH gene deficiency or inhibition on the modulation of inflammatory cytokines/chemokines and NF-κB signals as well VCAM-1 was measured using qPCR and Western blot approaches. The modulation of the eicosanoid metabolic profile was analyzed using a liquid chromatography/mass spectrometry (LC/MS–MS) method.

Methods and Materials

Animal Care, Breeding, and Genotyping

All animal experiments were approved by the Institutional Animal Care and Use Committee at Northwestern University. IL-10(−/−) mice in the C57BL/6J background were purchased from Jackson Laboratory. sEH(−/−) mice were originally described by Sinal et al. [19] and were extensively back bred into a C57BL/6 J background at the University of California, Davis, and were provided for this study.

In order to achieve double knockout sEH and IL-10 animals, Cross-breeding was performed with male IL-10(−/−) mice and female sEH(−/−) mice to generate IL-10(±)/sEH(±) double heterozygous litters. The IL-10(±)/sEH(±) littermates were further crossed to produce IL-10(−/−)/sEH(−/−) homozygous mice. All mice were housed in microisolator cages in the animal facilities at the Center for Comparative Medicine at Northwestern University in Chicago, IL. Genotyping of sEH was performed following the literature method [19, 22]. IL-10 genotyping was completed according to the Jackson Laboratory protocol.

Animal Experiments

The occurrence of spontaneous chronic active bowel inflammation varies greatly in mouse models of IBD in IL-10(−/−) mice [18]. In order to synchronize the development of chronic active bowel inflammation, five-week-old gender-matched IL-10(−/−), sEH(−/−)/IL-10(−/−), sEH(−/−), and wild-type mice were fed an AIN93 M diet containing 200 ppm of piroxicam (Sigma-Aldrich, St. Louis, MO) for one week [18]. After the one-week treatment with piroxicam, mice were then fed a purified AIN93M diet and tap water until the end of the experiment. Animals were sacrificed at either 10 days, 4 or 12 weeks after the induction/synchronization with piroxicam.

The second animal experiment was designed to determine the effects of the sEH inhibitor *t*-AUCB on inhibiting IBD activity in IL-10(−/−) mice. IL-10(−/−) mice (five-weeks old, both genders) were pre-treated with piroxicam

for one week to synchronize the development of IBD as described above [18]. The *t*-AUCB was synthesized in Dr. Hammock's Laboratory, and was administered to the mice ($n = 9$) via the drinking water four weeks after piroxicam induction. The animals were given 8 $mg \cdot L^{-1}$ *t*-AUCB containing 2.5 % polyethylene glycol 400 in drinking fluid for 4 weeks starting at the age of 9-weeks, and the experiment continued until week 13. The average animal body weight was 22–25 g, and the average fluid consumption per day was between 3-3.5 ml; therefore, the dose intake for *t*-AUCB was approximately 1 mg/kg. 2.5 % PEG 400 solution was given to the control mice ($n = 12$). All animals were sacrificed at week 13 after a four-week treatment course using *t*-AUCB.

Tissue Preparation and Histopathological Evaluation

Mice were euthanized by CO_2 asphyxiation. Colons, small intestines, and stomach were collected, opened longitudinally, and examined grossly. The entire opened gastrointestinal tract was fixed in 10 % buffered formalin, processed, and embedded in paraffin. Serial tissue sections (5 μm) were cut and mounted on glass slides for hematoxylin-eosin and immunohistochemical stains. Chronic active bowel inflammation was extensively analyzed histopathologically in serial H&E stained tissue sections. The degree of inflammation in the gastrointestinal tract was semi-quantitatively graded based on intensity of lymphocytes and plasma cells, regenerative/hyperplastic epithelial change, and ulcer formation following our established criteria [23].

Briefly, the intensity of lymphocyte and plasma cell infiltration in the lamina propria was graded as 0: less than 10 % lymphocytes and plasma cells, 1: 10–30 %, 2: 30–60 %, and 3: more than 60 %. Focal polypoid epithelial hyperplasia was graded as 0: no hyperplasia, 1: less than 20 % increased thickness of mucosa with mild elongated crypts (ratio of crypt length to mucosa thickness less that 30 %), 2: 20–50 % increased thickness of mucosa with moderately elongated crypts (ratio of crypt length to mucosa thickness 30–60 %), and 3: more than 50 % increased thickness of mucosa with markedly elongated crypts (ratio of crypt length to mucosa thickness >60 %). Ulceration was classified as the active ulcer which defined as mucosal ulcerative defect with adjacent epithelial hyperplastic reaction and the healed ulcer which defined as ulcerative defect mucosa was healed by polypoid epithelial hyperplasia/regeneration.

Immunohistochemistry

Immunohistochemical analysis was performed with antibodies against PCNA and myeloperoxidase in paraffin-embedded intestinal sections as previously described and details in the supplement [23–25]. The primary antibodies against PCNA (Mouse mAb, 2.5 μg/ml, Calbiochem, EMD Chemicals, Gibbstown, NJ) or anti-myeloperoxidase antibody (Rabbit pAb, 10 μg/ml, Abcam, Cambridge, MA) were applied to the tissue slides overnight at 4 °C. Anti-mouse or anti-rabbit IgG secondary antibodies (7.5 μg/ml) conjugated with ABC complexes (Avidin–Biotin-Complex, Vector Laboratories, Inc. Burlingame, CA) were incubated for 45 min at room temperature. Diaminobenzadine (Sigma–Aldrich, St. Louis, MO) was used as the chromogen. Slides were counterstained with Mayer's hematoxylin for 30 s. Positively staining cells were scored (at least five randomly selected fields and > 500 cells counted) and reported as mean ± SD.

Biochemical Analysis of Plasma Eicosanoid Profile and *t*-AUCB Using a Liquid Chromatography/Tandem Mass Spectrometry (LC/MS–MS) Method

Serum specimens were spiked with 10 μl of 50 nM internal standard I and were extracted by solid phase extraction using Oasis HLB cartridges. LC/MS–MS analysis of eicosanoid profile and *t*-AUCB was performed using a modified method based on the previous publications and details in the supplement [26].

Quantitative PCR Assay

mRNA expression was determined using the two-step q-RT-PCR assay. The region of IFN-gamma, TNF-alpha, MCP-1, and VCAM-1 mRNA were amplified using the well-designed primers [27, 28]. GAPDH (Glyceraldehyde-3-phosphate dehydrogenase) was used as internal control. Data for each mRNA expression were shown as the relative fold of change normalized by that of GAPDH.

Western Blotting

The whole tissue/cell lysates of the colon mucosa samples from mice underwent SDS–polyacrylamide gel (4–12 % gradient) electrophoresis. The resolved proteins were transferred onto a polyvinylidene fluoride membrane and probed with the primary antibody including anti-phosphorylated NF-κB P65 (S276), anti-Iκκ-α, and anti-mouse ß-actin mAb. The specific signals were visualized by enhanced chemiluminesence.

Statistical Analysis

Each analyzed parameter was expressed as Mean ± SD, unless otherwise stated, with at least three independent measurements. Continuous variables were compared using

the Student's *t*-test, whereas categorical variables were compared using Chi-square test. All statistical tests were two-sided, and statistical significance was taken as $p < 0.05$.

Results

Development of sEH(−/−)/IL-10(−/−) Mice and General Animal Data

To determine the role of the sEH gene on active inflammatory process in IL-10 (−/−) mice, a deficiency of the sEH gene in IL-10 (−/−) mice was developed. The double knockout sEH(−/−)/IL-10(−/−) mice did not display any gross abnormalities and showed a similar breeding ability as IL-10(−/−) mice. Body weights (measured weekly) did not reveal any significant differences between the female double knockout sEH(−/−)/IL-10(−/−) mice and IL-10(−/−) mice; however, a marked reduction of body weight was observed between the male sEH(−/−)/IL-10(−/−) mice and IL-10(−/−) mice. At the beginning of the experiment, the average body weight of male IL-10 (−/−) animals was lower than that of male sEH(−/−)/IL-10 (−/−) animals (20.2 ± 1.5 g vs. 22.1 ± 1.6 g). However, at 6 weeks after piroxicam induction, average body weight of male sEH(−/−)/IL-10 (−/−) animals began to stop growth, and at the time of the 7th week, it was caught up by male IL-10 (−/−) mice. At the ending point of the experiment, the body weight of male sEH(−/−)/IL-10 (−/−) mice (23.9 ± 2.5 g) was reduced nearly 15 %, and significantly lower than that of male IL-10 (−/−) group (26.5 ± 1.3 g, $p < 0.05$, as seen in Fig. 1 supple in the supplemented data). Food and water consumption did not reveal any differences in the double knockout sEH(−/−)/IL-10(−/−) mice as compared to the controls.

Effect of sEH Gene Deficiency or Inhibition on Chronic Active Inflammation in the Gastrointestinal Tract

In order to synchronize the development of IBD, the mice were fed an AIN93 M diet containing 200 ppm of piroxicam for one week [18]. Early mucosal injury in the bowel was observed 10 days after piroxicam use; sEH(−/−)/IL-10(−/−) mice, sEH(−/−) mice, and wild-type control animals all exhibited mild mucosal ulcer formation in the cecum and proximal small bowl. sEH(−/−)/IL-10(−/−) and sEH(−/−) mice showed much milder ulcerations as compared to the IL-10(−/−) mice. While the sEH(−/−) and wild-type control mice showed a full recovery from the erosion and ulceration 4 weeks after piroxicam use, the sEH(−/−)/IL-10(−/−) and IL-10(−/−) mice continued to display chronic active IBD ($n = 3$ mice each strain each gender mice). Thus, the IBD process was synchronically induced in the sEH(−/−)/IL-10(−/−) and IL-10(−/−) mice at four weeks post-piroxicam treatment.

Extensive histopathological analysis for chronic active inflammation in the bowel was performed at 12 weeks post-piroxicam induction. No inflammation was identified in the control sEH(−/−) or wild-type mice. In the IL-10(−/−) mice, active IBD was observed and presented as focal active ulceration (ulcerative defect in the mucosa with adjacent epithelial hyperplastic reaction), as seen in Fig. 1a, and transmural inflammation (inflammatory cells infiltrating into the muscularis propria and subserosa), as seen Fig. 1d. As seen in histogram Fig. 1g, h, 73 % (8/11) IL-10(−/−) mice exhibited active ulcer, and 90.0 % (10/11) displayed focal transmural inflammation. Double knockout sEH(−/−)/IL-10(−/−) mice only displayed focal mild chronic active inflammation and healed ulcer with polypoid epithelial hyperplasia in the bowel (Fig. 1b, e). Although 71 % (10/14) mice had overall ulcer formation (including healed and active ulcers), most of the ulcers were the healed ulcers which was defined as ulcerative defect mucosa was healed by polypoid epithelial hyperplasia/regeneration (Fig. 1b). Significant reduction of active ulcer formation and transmural inflammation were observed in sEH(−/−)/IL-10(−/−) mice; and as seen in Fig. 1g, h, only 29 % (4/14) sEH(−/−)/IL-10(−/−) mice had small active ulcer ($p < 0.05$) and 43 % (6/14) exhibited mild transmural inflammation in the cecum ($p < 0.05$). Compared to IL-10(−/−) mice, treatment with *t*-AUCB showed similar results as those seen in sEH(−/−)/IL-10(−/−) mice and resulted in a significant reduction of active ulcer formation [22.2 % (2/9 mice), $p < 0.05$] and transmural inflammation in the bowel [44 % (4/9), $p < 0.05$], as seen in Fig. 1c, f, and histogram Fig. 1g, h.

Neutrophil infiltration into the lamina propria, intestinal epithelium (cryptitis), and luminal surface (crypt abscess) are crucial morphologic parameters for inflammatory activity in IBD. Immunohistochemical analysis of neutrophil infiltration was performed with antibodies against myeloperoxidase (MPO) [29]. MPO-positive cells were rarely observed in morphologically normal mucosa, but frequently seen in active inflammatory areas (Fig. 2a). Intense MPO- positive cells were seen in the inflamed intestinal mucosa in IL-10(−/−) mice (Fig. 2a), and a markedly decreased intensity of MPO-positive cells was found in sEH(−/−)/IL-10(−/−) mice (Fig. 2b) and IL-10(−/−) mice treated with *t*-AUCB (Fig. 2c). The density of MPO-positive cell was determined and expressed as mean numbers of positive cells per high power field (40×) in the inflamed areas. The results showed that the MPO-positive cells in the inflamed areas was significantly lower in sEH(−/−)/IL-10(−/−) mice (Fig. 2d) and IL-10(−/−) mice treated with *t*-AUCB (Fig. 2e) as compared to IL-10(−/−) mice ($p < 0.01$).

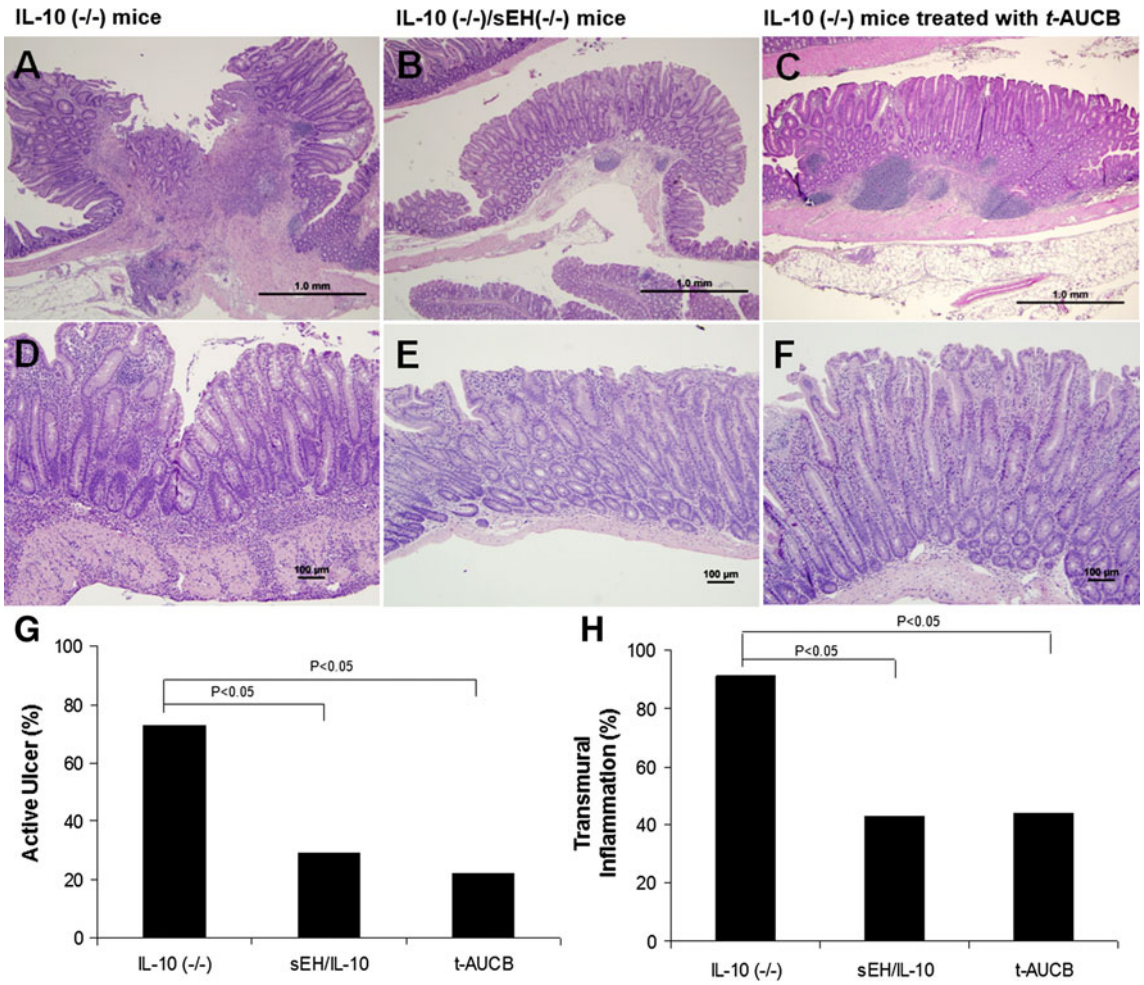

Fig. 1 Histopathologic analysis of inflammatory activity in the bowel in IL-10(−/−) mice, sEH (−/−)/IL-10(−/−) mice, and IL-10(−/−) mice treated with *t*-AUCB: **a** active ulcer in the colon in IL-10(−/−) mice; **b** and **c** a healed ulcer with hyperplasic/regenerative epithelium in sEH (−/−)/IL-10(−/−) mice and IL-10(−/−) mice treated with *t*-AUCB, respectively; **d** active transmural inflammation and epithelial hyperplastic change in IL-10(−/−) mice; **e** and **f** mild lymphocyte and plasma cells in lamina propria and hyperplastic epithelial change but no or minimal transmural inflammation in sEH (−/−)/IL-10(−/−) mice and IL-10(−/−) mice treated with *t*-AUCB, respectively. **g** and **h** Histogram of active ulcer formation and transmural inflammation scores in IBD in IL-10(−/−) and sEH(−/−)/IL-10(−/−) mice as well as in IL-10(−/−) mice treated with *t*-AUCB. The statistically significant difference between IL-10(−/−) and sEH(−/−)/IL-10 (−/−) mice as well between IL-10(−/−) mice and IL-10(−/−) mice treated with *t*-AUCB were marked in the histogram

The overall intensity of inflammatory cell infiltrates (prominent lymphocytes and plasma cells) or called lymphoplasmacytosis in the lamina propria in the bowel was further semi-quantitatively analyzed. As seen in the histogram Fig. 2f, g, the density of inflammatory cell infiltration was significantly decreased in the bowel in sEH(−/−)/IL-10(−/−) mice and IL-10(−/−) mice treated with *t*-AUCB as compared to IL-10(−/−) mice ($p < 0.05$).

sEH Deficiency or Inhibition Did Not Affect Cell Proliferation for the Healing/Regeneration Process

Whether sEH gene deficiency or inhibition affect epithelial regeneration and healing process in the active inflammation was further analyzed for PCNA-labeled cell proliferation and epithelial regenerative hyperplasia. As seen in Fig. 3a–d, PCNA-labeled cell proliferation in morphologically normal mucosa in the colon in all of four genotype mice (wild-type, sEH(−/−), IL-10(−/−), and sEH(−/−)/IL-10(−/−) mice) was similar and showed PCNA-labeled proliferative cells located in the crypt only. PCNA-labeled cell proliferation markedly increased in focal polypoid hyperplastic/regenerative epithelia adjacent to ulcers in IL-10(−/−) mice (Fig. 3e) and in sEH(−/−)/IL-10(−/−) mice (Fig. 3f) as compared to normal mucosa. The proliferation index was determined by counting (%) of the PCNA-positive cells within areas of focal polypoid hyperplasia in the intestine. PCNA-labeled proliferation

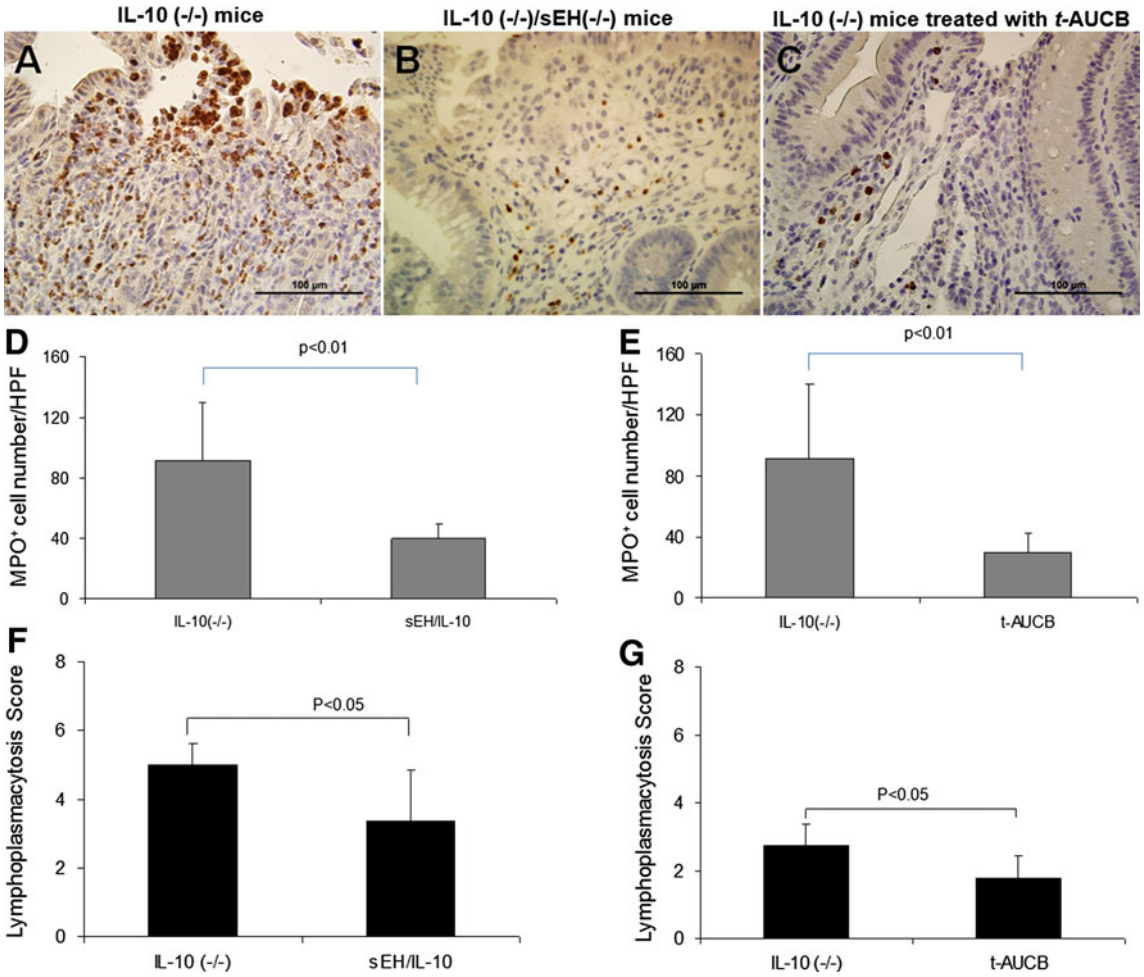

Fig. 2 Immunohistochemical staining of myeloperoxidase (MPO)-labeled neutrophils: **a**–**c** MPO-positive cells in the inflamed colonic mucosa in IL-10(−/−) mice, sEH(−/−)/IL-10(−/−) mice, and IL-10(−/−) mice treated with *t*-AUCB, respectively. **d**, **e** Histogram of semi-quantitative analysis of MPO-positive cells in the inflamed mucosa: the number of MPO-positive cells was expressed as Mean ± SD. **f**, **g** Histogram of semi-quantitative analysis of lymphoplasmacytosis in the inflamed colonic mucosa in IBD mice. Statistically significant difference between IL-10(−/−) and sEH(−/−)/IL-10(−/−) mice as well between IL-10(−/−) mice and IL-10(−/−) mice treated with *t*-AUCB were marked in the histograms

index were minimally increased in the hyperplastic/regenerative epithelia in sEH (−/−)/IL-10(−/−) mice (49.6 ± 4.1 %, $p = 0.18$) and IL-10 (−/−) mice treated with *t*-AUCB (52.2 ± 4.1 %, $p = 0.12$) as compared to the hyperplastic/regenerative epithelia in IL-10(−/−) mice (44.4 ± 5.2 %), but did not have statistical significance.

Focal polypoid epithelial hyperplasia/regeneration was further semi-quantitatively analyzed and showed that there was no difference in focal polypoid epithelial hyperplasia/regeneration in the sEH(−/−)/IL-10(−/−) mice (2.93 ± 1.07) compared to IL-10(−/−) mice (3.27 ± 1.01, $p = 0.4$). Same trend was observed in IL-10(−/−) mice treated with *t*-AUCB (1.44 ± 0.53) as compared to IL-10(−/−) mice (2.08 ± 0.52, $p = 0.12$).

sEH Deficiency or Inhibition Suppresses Inflammatory Cytokines, Chemokines, and NF-kB Signaling

Freshly collected colonic mucosa ($n = 11$/group, both genders) were analyzed for the fold change of mRNA expression of inflammatory cytokines, chemokines, and VCAM-1 using a quantitative real-time PCR assay. As shown in Fig. 4a, b, compared to wild type mice and sEH(−/−) mice, a significant increase of IFN-γ, TNF-α, and MCP-1 and VCAM-1 mRNA expressions were observed in the colonic mucosa of IL-10(−/−) mice ($p < 0.01$). Compared to IL-10 (−/−) IBD mice, sEH(−/−)/IL-10(−/−) mice exhibited a statistically significant decrease of IFN-γ, TNF-α, MCP-1, and VCAM-1 mRNA expression was observed as compared to IL-10(−/−) mice ($p < 0.05$). In

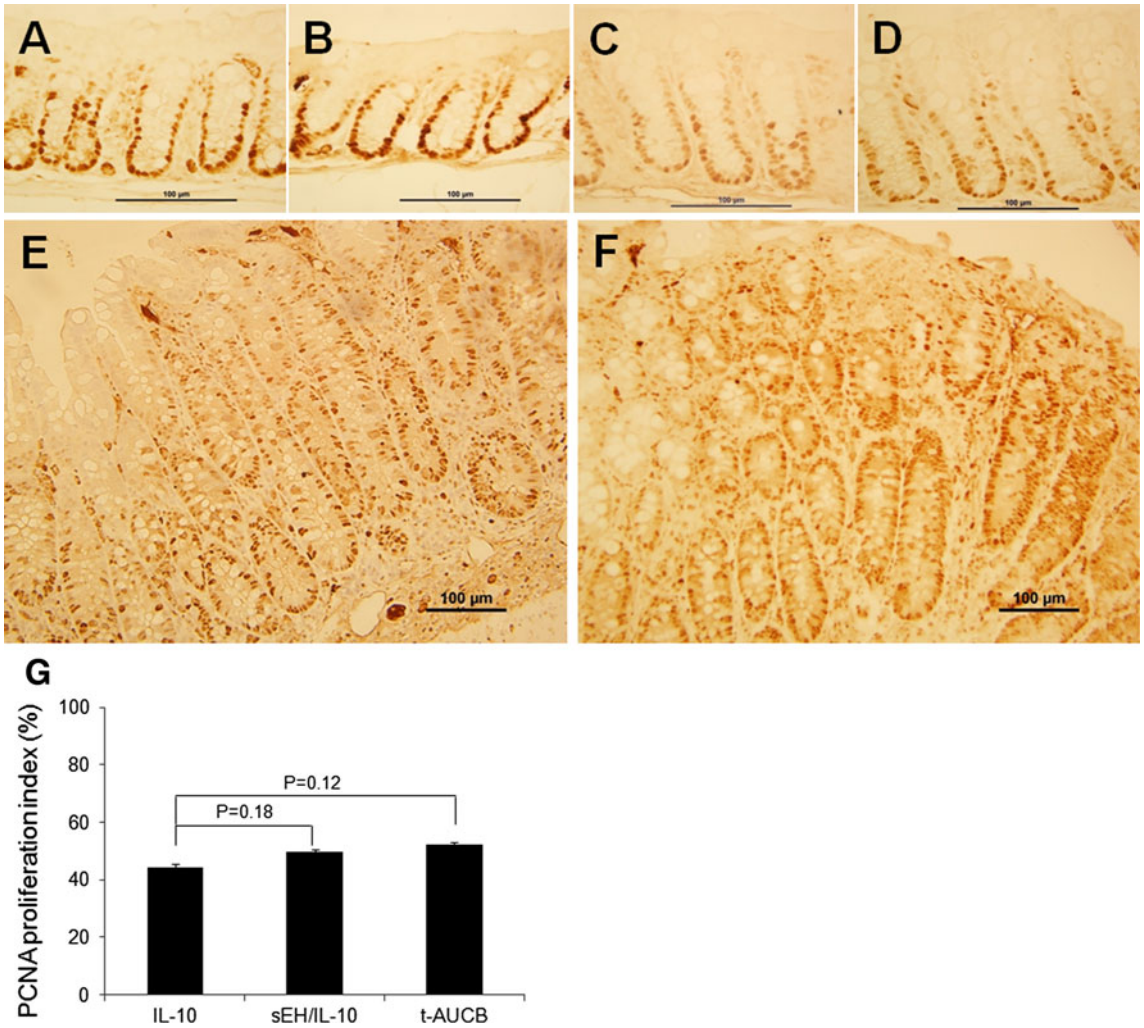

Fig. 3 Immunohistochemical staining of PCNA-labeled cell proliferation: **a**–**d** PCNA-labeled proliferative cells in morphologically normal colonic mucosa in wild type mice (**a**), sEH(−/−) mice (**b**), IL-10(−/−) mice (**c**), and sEH(−/−)/IL-10(−/−) mice (**d**); **e**, **f** PCNA-labeled proliferative cells in hyperplasic mucosa adjacent to ulcer in IL-10(−/−) mice (**e**) and in sEH(−/−)/IL-10(−/−) mice (**f**). **g** Histogram of PCNA proliferation index in the inflamed colonic mucosa in IBD in IL-10(−/−) mice compared to sEH(−/−)/IL-10(−/−) mice and IL-10(−/−) mice treated with *t*-AUCB. Statistically significant difference between IL-10(−/−) and sEH(−/−)/IL-10(−/−) mice as well between IL-10(−/−) mice and IL-10(−/−) mice treated with *t*-AUCB were marked in the histograms

IL-10(−/−) mice treated with *t*-AUCB, a statistically significant decrease of IFN-γ, MCP-1, and VCAM-1 mRNA expression was found ($p < 0.05$), but not TNF-α, as compared to IL-10(−/−) mice. There was no statistical difference observed between wild type mice and sEH(−/−) mice.

Using a western blot approach with whole tissue lysates and a β-actin as the internal protein control, the expression intensity of phosphorylated NF-kB p65 (S276) and Ikk-α proteins as well VCAM1 in the colonic mucosa showed a marked decrease (Fig. 4c). The expression intensity of these signals was determined and displayed a statistically significant decrease in sEH(−/−)/IL-10(−/−) mice as compared to IL-10(−/−) mice (Fig. 4d–f). Obviously, colitis mucosa in IL-10(−/−) mice exhibited a significantly increase of these signals as compared to wild type mice and sEH(−/−) mice (Fig. 4c–f).

Effects of sEH Deficiency or Inhibition on Modulating Eicosanoid Profile and *t*-AUCB Plasma Levels Analyzed by A LC/MS–MS Assay

Simply, the ratios of epoxide eicosanoids to their corresponding diols (EpOMEs to DiHOMEs) and EETs to DHETs are the most commonly used biomarkers for determining sEH inhibition or gene deficiency; and these ratios are efficiently analyzed by a LC/MS–MS assay [10]. As seen in the left two panels of Fig. 5a, compared to IL-10(−/−) mice, sEH(−/−)/IL-10(−/−) mice exhibited a highly significant increase of ratios of EpOMEs to

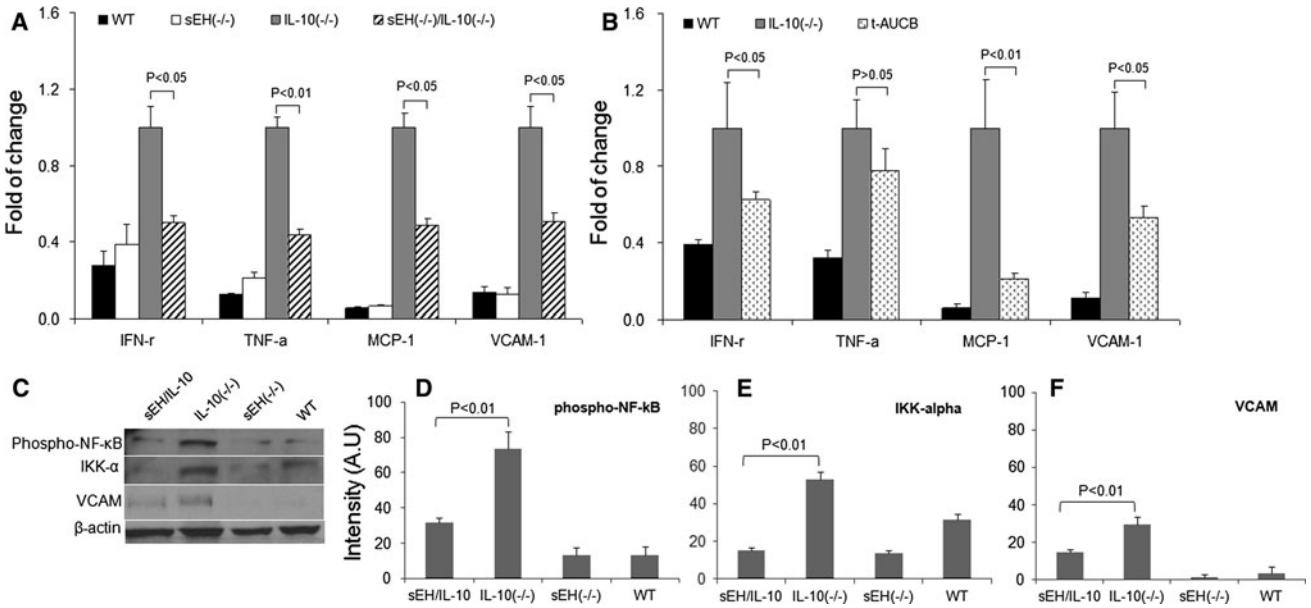

Fig. 4 Analysis of IFN-γ, TNF-α, and MCP-1 as well VCAM-1 mRNA expressions using quantitative real-time PCR and assay of NF-κB signaling using western blot approach: IFN-γ, TNF-α, and MCP-1 as well VCAM-1 mRNA expressions in wild type, sEH(−/−), IL-10(−/−) and sEH(−/−)/IL-10(−/−) mice (**a**); and in wild type mice, IL-10(−/−) mice and IL-10(−/−) mice treated with *t*-AUCB (**b**). Western blot assay for phosphorylated NF-kB p65 (S276) and Ikk-α as well VCAM-1 in sEH(−/−)/IL-10(−/−), IL-10(−/−), sEH(−/−), and wild type mice (**c**), and quantitative densitometry analysis of phosphorylated NF-kB p65 (S276) and Ikk-α as well VCAM-1 (**d**–**f**). Statistically significant difference of these cytokines and NF-κB signals either in IL-10(−/−) mice compared to sEH(−/−)/IL-10(−/−) mice or in IL-10(−/−) mice compared to IL-10(−/−) mice treated with *t*-AUCB was marked in the histogram figures

DiHOMEs and EETs to DHETs ($p < 0.001$). By further analyzing sEH predominantly metabolized 14(15) EET and its corresponding 14(15)DHET, as well as epoxide eicosanoids and their corresponding diols (DiHOMEs), the stabilized/increased levels of 14(15) EET and EpOMEs, and decreased levels of 14(15)DHET and DiHOMEs were found in sEH(−/−)/IL-10(−/−) mice as compared to IL-10(−/−) mice. A similar trend was observed in other epoxide products and their corresponding diols; these products include epoxide eicosanoids [5(6)-, 8(9)-, and 11(12)-EET], EpOME [9(10)- and 12(13)-EpOME], the diol products [9(11)-DiHOME and 12(13)-DiHOME, 5(6)-DHET, 8(9)-DHET, and 11(12)-DHET]. As seen in the right panel of Fig. 5b, similar patterns of the changes of these ratios were observed in IL-10(−/−) mice treated with *t*-AUCB as compared to IL-10(−/−) mice, and showed a significant increased ratio of EETs to DHETs ($p < 0.05$), as well as increased level of 14(15) EET ($p < 0.05$). In the left panel of Fig. 5a, a similar pattern of changes of these ratios was also observed in sEH(−/−) mice as compared to wild type mice.

To investigate whether the sEH gene deficiency or inhibition modulates other pathways of arachidonic acid metabolism, particularly in the cyclooxygenase (COX2) and 5-lipoxygenase (5-LOX)-mediated pathways, the key metabolites involved in these pathways were analyzed. As shown in Fig. 6a, the levels of LTB_4 (Leukotriene B4) and 5-HETE (hydroxyeicosatetraenoic acid) as the products of 5-LOX pathway and PGE2 (prostaglandin E2, COX-2 mediated product) were markedly decreased in sEH(−/−)/IL-10(−/−) mice as compared to IL-10 (−/−) mice, but not reached statistically significant ($p > 0.05$). Similarly, the levels of PGE_2, LTB4 and 5-HETE showed slightly difference in sEH(−/−) mice as compared to wild type mice, but no statistical difference (Fig. 6a). In Fig. 6b, IL-10(−/−) mice treated with *t*-AUCB also exhibited the slightly decreased levels of PGE2, LTB4, and 5-HETE, but not reached statistical significance as compared to IL-10 (−/−) mice.

Plasma level of *t*-AUCB was also analyzed using a LC/MS–MS assay and showed average level of *t*-AUCB was 2.63 ± 2.34 nM and ranged from 0.43 nM to 7.76nM.

Discussion

The human sEH is encoded by the EPHX-2 gene. The EPHX-2 gene-encoded product has an *N*-terminal domain that contains lipid phosphatase activity [30, 31] and a carboxy-terminal domain with epoxide hydrolase activity. The bifunctional nature of the EPHX-2 encoded protein allows for inhibition of one domain with no effect on the enzymatic activity of the other domain. The role of the *c*-terminal epoxide hydrolase in inflammation has been

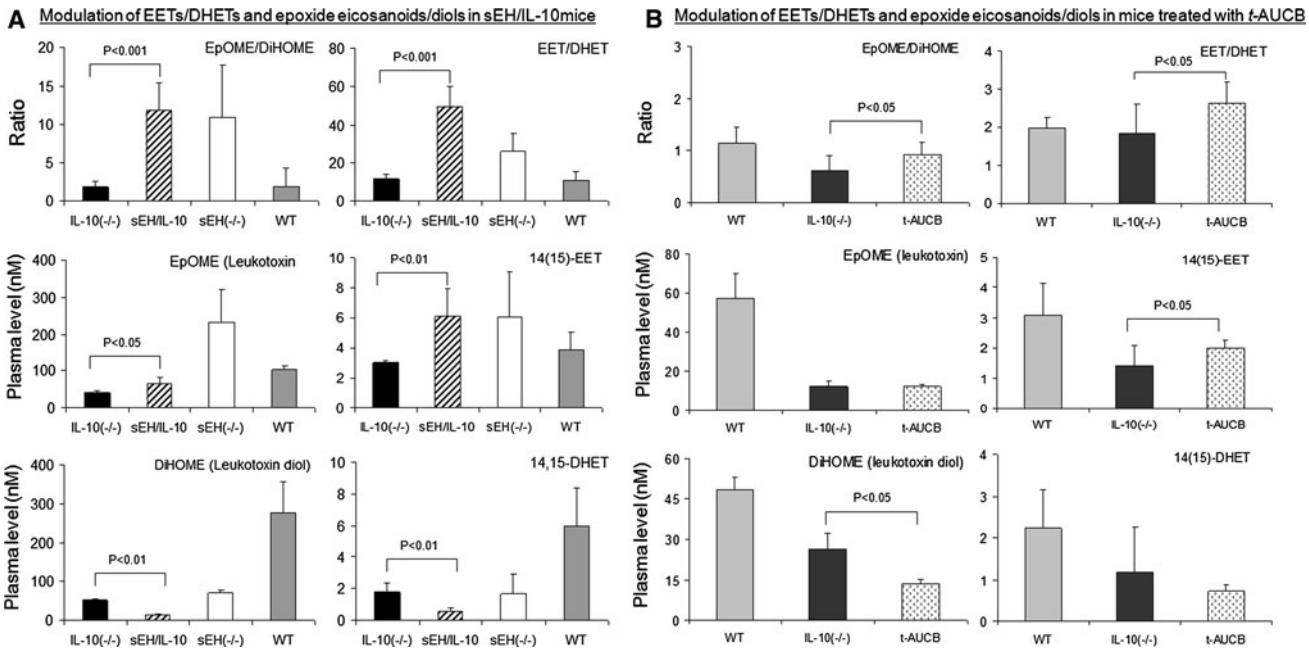

Fig. 5 Analysis of plasma levels of epoxygenase-dependent metabolites using a *LC/MS/MS* assay: The difference of the ratios of total EpOME to DiHOME and EETs to DHETs, and the concentration (nM, Mean ± SD) of EpOMEs (including 9(10)- and 12(13)-EpOME), DiHOMEs (including 9(11)-DHOME and 12(13)-DHOME), 14(15)-EET, and 14(15)-DHET among IL-10(−/−), sEH(−/−)/IL-10(−/−), sEH(−/−), and wild type (wt) mice (**a**) as well among wild type (wt) mice, IL-10(−/−) mice, and IL-10(−/−) mice treated with *t*-AUCB (**b**). Statistically significant difference of these metabolites either in sEH(−/−)/IL-10(−/−) mice compared to IL-10(−/−) mice (**a**, left two panels of histograms) or in IL-10(−/−) mice compared to IL-10(−/−) mice treated with *t*-AUCB (**b**, right two panels of histograms) was marked in the figures

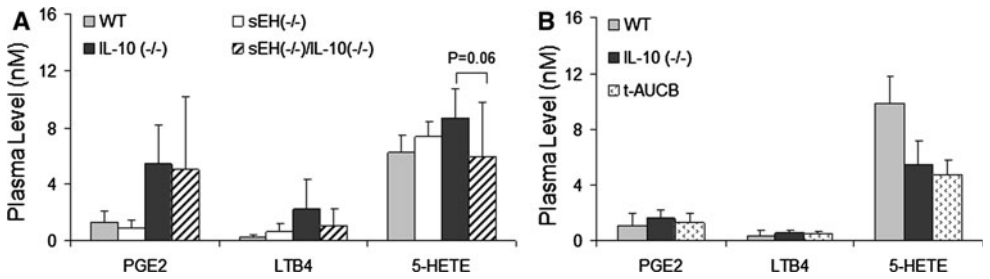

Fig. 6 Analysis of plasma levels of *COX-2 and 5-LOX*-dependent metabolites using a *LC/MS–MS* assay: the concentration (nM, Mean ± SD) of PGE_2, LTB_4, and 5-HETE in wild type (wt) mice, sEH(−/−), IL-10(−/−), and sEH(−/−)/IL-10(−/−) mice (**a**), and in wild type (wt) mice, IL-10(−/−) mice, and IL-10(−/−) mice treated with *t*-AUCB (**b**)

preliminarily assessed in rodent models [2]. sEH hydrolyzes EETs to their much less biologically active DHETs, dramatically reducing anti-inflammatory activity of EETs [1]. Isoprenoid pyro- and monophosphates are substrates for the *N*-terminal phosphatase domain [31, 32] and these lipid phosphates are the metabolic precursors of cholesterol biosynthesis, and most importantly they are used for isoprenylation, a protein post-translational lipid modification process that is involved in the process of inflammation [33–35]. In the present study, using an advanced approach of the IBD model in IL-10(−/−) mice combined with sEH/EPHX-2 gene deficiency or sEH inhibition, we demonstrated that sEH gene deficiency or inhibition significantly ameliorated chronic active inflammation in the bowel, particularly reduced active ulcer formation, trnasmural inflammation, and inflammatory cell infiltration.

The neutrophil crytitis and crypt abscesses are key pathogenic events in the disease activity in IBD. The intense infiltration of leukocytes along with the overproduction of reactive oxygen and nitric oxide free radicals, inflammatory cytokines/chemokines, and arachidonic acid metabolites are the key contributory factors to inflammatory activity and inflammatory injury in the bowel. It has been demonstrated that physiologic concentrations of EETs decrease the expression of endothelial cell adhesion molecules such as VCAM-1 (induced by TNF-α via NF-κB)

and thus prevent subsequent leukocyte adhesion to the vascular wall and reduce inflammatory cell infiltration into the inflamed tissues [2]. sEH, as a pro-inflammatory enzyme, converts EETs to DHETs that inactivate anti-inflammatory function of EETs. In this study, we demonstrated a significant reduction in the intensity of MPO-labeled neutrophils and lymphoplasmacytosis in IBD in sEH(−/−)/IL-10(−/−) mice, as well as in IL-10(−/−) mice treated with the sEH inhibitor *t*-AUCB. These results indicate that the inhibition of inflammatory activity, particularly neutrophil infiltration, is a major anti-inflammatory event by sEH inhibition.

The infiltration of inflammatory cells is mediated in part via pro-inflammatory cytokines and chemokines. TNF-α, a central inflammatory cytokine, involves in both systemic inflammation and the stimulation of the acute phase reaction. TNF-α promotes the inflammatory response and causes many of the clinical problems associated with idiopathic inflammatory disorders such as IBD. TNF-α together with other cytokines and chemokines including interferon-γ (IFN-γ) and monocyte chemotactic protein-1 (MCP-1) plays crucial role in stimulating a proinflammatory cytokine produced by Th1 cells [36], inducing the expression of integrins and VCAM-1 required for chemotaxis, and acting as a potent attractant for inflammatory cells (monocytes and lymphocytes) [37]. Particularly, VCAM-1 induced by TNF-α via NF-κB is important for leukocyte adhesion to the vascular wall and infiltrating into inflamed tissues [2]. Our results revealed that the levels of TNF-α, IFN-γ, and MCP-1 as well as VCAM-1 in the inflamed colonic tissues were significantly decreased in sEH(−/−)/IL-10(−/−) mice and in IL-10(−/−) mice treated with *t*-AUCB. Furthermore, Ikk-α and phosphorylated NF-κB were significantly down-regulated in sEH(−/−)/IL-10(−/−) mice. These findings suggest that the suppression of these inflammatory cytokines and chemokines as well as NF-κB signaling by sEH gene deficiency or inhibition are key mechanism in suppressing inflammatory activity in IBD.

One of the pivotal molecules in inflammation is arachidonic acid, which simplistically has three potential metabolic fates, including cyclooxygenase (COX), lipoxygenase (LOX), and cytochrome P450 epoxygenases mediated metabolic pathways to generate biologically active mediators involved in the inflammatory cascade. A LC/MS–MS method is highly efficient approach to analyze endogenous lipid mediators [38] and facilitates the quantitative analysis of over 120 eicosanoid metabolites using an ABI linear trap instrument in MRM mode [39, 40]. This "omic" approach provides much more insight than can be obtained from monitoring a single analyte such as EET or DHET and provide an opportunity on understanding the interactions among three arachidonic acid metabolic pathways via targeting the key enzyme/s. Similar to the previous studies using sEH inhibitors [10], a simple biomarker for monitoring the effect of sEH inhibition is the ratio of lipid epoxides to diols. As expected, sEH gene deficiency or sEH inhibition resulted in a significant increase in the ratios of EETs/DHETs and EpOMEs/DiHOMEs, confirming the known function of sEH in metabolizing epoxide products, particularly converting 14(15) EET to 14(15) DHET. Analysis of the eicosanoid profile further revealed that sEH gene deficiency displayed a marked reduction of the LTB4 and 5-HETE metabolites when compared to IL-10(−/−) mice. These results simply imply that sEH gene deficiency shifts the eicosanoid profile from propagation of inflammation to its resolution in which LTB_4 and HETEs stimulate inflammatory cell activities and PGE_2 participates in regeneration and ulcer healing. But, *t*-AUCB, sEH inhibitor, appears not as strong as sEH gene deficiency in modulation of these metabolic pathways.

The clinical use of nonsteroidal anti-inflammatory drugs (NSAIDs) exacerbates inflammatory bowel disease (IBD) [41]. NSAIDs and COX-2-specific inhibitors (e.g., celecoxib) have been shown to be harmful in animal models of IBD as well [42, 43]. These findings may be explained by the idea that 1) COX2 and PGE_2 inhibition leads to inhibition of cell proliferation and a delay in ulcer healing and 2) leads to shunting of arachidonic acid substrates to other pathways, particularly to the 5-LOX pathway [44–47]. Here, sEH gene deficiency or inhibition results in slightly decreased level of LTB_4 and 5-HETE and no significant change on PGE2, indicating that direct targeting of sEH would be different from NSAIDs and may even overcome the toxicity of NSAIDs to IBD. In particular, shifting the eicosanoid profile from propagation of inflammation (LTB4 and HETEs) to EETs and the PGE2-led regenerative healing process could prove beneficial for the treatment of IBD.

The results of the eicosanoid profiling also correlate well with the morphological inflammatory activities in the bowels. LTB_4 and 5-HETE are well known pro-inflammatory mediators that are able to induce inflammatory cell infiltration by inducing adhesion and activation of leukocytes on the endothelium, allowing them to bind to and cross it into the inflamed tissue [48]. Down-regulation of the levels of LTB_4 and 5-HETE is also a partial mechanism of reduction of MPO-labeled inflammatory cell infiltration in sEH(−/−)/IL-10(−/−) mice in addition to lowering inflammatory cytokines and chemokines. Whether or not the modulation of the eicosanoid profile by sEH gene deficiency or inhibition is involved in regulation of inflammatory cytokines need to be investigated further.

t-AUCB is a potent sEH inhibitor with IC_{50} of sEH inhibition 1.5 ± 0.2 nM. LC/MS–MS based analytical

procedures allow to detect picomolar concentrations of the sEH inhibitors including *t*-AUCB from ~ 5 μl of blood, and to perform the rapid ADME studies. Herein, we have demonstrated that administration of 8 mg/liter *t*-AUCB to mice in drinking fluid reached to 2.63 ± 2.34 nM plasma levels which was within the range of IC_{50} sEH inhibition and showed the inhibitory effect on inflammation in the bowel. Thus, *t*-AUCB will be highly potential for treating IBD in human in future.

To conclude, the sEH gene deficiency or inhibition results in a significant reduction in inflammatory cell infiltration and active ulcer formation in IBD in IL-10(−/−) mice, as well as decreased inflammatory cytokine expression and shifting of the eicosanoid profile from propagation of inflammation to its resolution. These findings indicate that sEH involves in the process of inflammation in IBD and thus is a potential target for the treatment of IBD.

Acknowledgments This study was supported by NIH R01 CA137467 to GYY. Partial supports were provided by NIEHS R01 ES002710 and NIEHS Superfund Program P42 ES004699. BDH is a George and Judy Marcus Senior Fellow of The American Asthma Foundation.

Conflict of interest None.

References

1. Inceoglu B, Schmelzer KR, Morisseau C, Jinks SL, Hammock BD. Soluble epoxide hydrolase inhibition reveals novel biological functions of epoxyeicosatrienoic acids (EETs). *Prostaglandins Other Lipid Mediat*. 2007;82:42–49.
2. Node K, Huo Y, Ruan X, et al. Anti-inflammatory properties of cytochrome P450 epoxygenase-derived eicosanoids. *Science*. 1999;285:1276–1279.
3. Chiamvimonvat N, Ho CM, Tsai HJ, Hammock BD. The soluble epoxide hydrolase as a pharmaceutical target for hypertension. *J Cardiovasc Pharmacol*. 2007;50:225–237.
4. Huang H, Morisseau C, Wang J, et al. Increasing or stabilizing renal epoxyeicosatrienoic acid production attenuates abnormal renal function and hypertension in obese rats. *Am J Physiol Renal Physiol*. 2007;293:F342–F349.
5. Zhang W, Koerner IP, Noppens R, et al. Soluble epoxide hydrolase: a novel therapeutic target in stroke. *J Cereb Blood Flow Metab*. 2007;27:1931–1940.
6. Schmelzer KR, Kubala L, Newman JW, Kim IH, Eiserich JP, Hammock BD. Soluble epoxide hydrolase is a therapeutic target for acute inflammation. *Proc Natl Acad Sci USA*. 2005;102:9772–9777.
7. Smith KR, Pinkerton KE, Watanabe T, Pedersen TL, Ma SJ, Hammock BD. Attenuation of tobacco smoke-induced lung inflammation by treatment with a soluble epoxide hydrolase inhibitor. *Proc Natl Acad Sci USA*. 2005;102:2186–2191.
8. Zhao X, Yamamoto T, Newman JW, et al. Soluble epoxide hydrolase inhibition protects the kidney from hypertension-induced damage. *J Am Soc Nephrol*. 2004;15:1244–1253.
9. Fleming I. DiscrEET regulators of homeostasis: epoxyeicosatrienoic acids, cytochrome P450 epoxygenases and vascular inflammation. *Trends Pharmacol Sci*. 2007;28:448–452.
10. Liu JY, Tsai HJ, Hwang SH, Jones PD, Morisseau C, Hammock BD. Pharmacokinetic optimization of four soluble epoxide hydrolase inhibitors for use in a murine model of inflammation. *Br J Pharmacol*. 2009;156:284–296.
11. Liu JY, Yang J, Inceoglu B, et al. Inhibition of soluble epoxide hydrolase enhances the anti-inflammatory effects of aspirin and 5-lipoxygenase activation protein inhibitor in a murine model. *Biochem Pharmacol*. 79:880–887.
12. Inceoglu B, Jinks SL, Schmelzer KR, Waite T, Kim IH, Hammock BD. Inhibition of soluble epoxide hydrolase reduces LPS-induced thermal hyperalgesia and mechanical allodynia in a rat model of inflammatory pain. *Life Sci*. 2006;79:2311–2319.
13. Colombel JF, Watson AJ, Neurath MF. The 10 remaining mysteries of inflammatory bowel disease. *Gut*. 2008;57:429–433.
14. Russel MGVM, Stockbrugger RW. Epidemiology of inflammatory bowel disease: an update. *Scand J Gastroenterol*. 1996;31:417–427.
15. Langman MJS. Epidemiological overview of inflammatory bowel disease. In: Allan RN, Rhodes JM, Hanauer SB, Keighley MRB, Alexander-Williams J, Fazio VW, eds. *Inflammatory Bowel Diseases*. New York: Churchill Livingstone; 1997:35–39.
16. Noble A, Baldassano R, Mamula P. Novel therapeutic options in the inflammatory bowel disease world. *Dig Liver Dis*. 2008;40:22–31.
17. Kuhn R, Lohler J, Rennick D, Rajewsky K, Muller W. Interleukin-10-deficient mice develop chronic enterocolitis. *Cell*. 1993;75:263–274.
18. Narushima S, Spitz DR, Oberley LW, et al. Evidence for oxidative stress in NSAID-induced colitis in IL10−/− mice. *Free Radic Biol Med*. 2003;34:1153–1166.
19. Sinal CJ, Miyata M, Tohkin M, Nagata K, Bend JR, Gonzalez FJ. Targeted disruption of soluble epoxide hydrolase reveals a role in blood pressure regulation. *J Biol Chem*. 2000;275:40504–40510.
20. Manhiani M, Quigley JE, Knight SF, et al. Soluble epoxide hydrolase gene deletion attenuates renal injury and inflammation with DOCA-salt hypertension. *Am J Physiol Renal Physiol*. 2009;297:F740–F748.
21. Motoki A, Merkel MJ, Packwood WH, et al. Soluble epoxide hydrolase inhibition and gene deletion are protective against myocardial ischemia-reperfusion injury in vivo. *Am J Physiol Heart Circ Physiol*. 2008;295:H2128–H2134.
22. Luria A, Bettaieb A, Xi Y, et al. Soluble epoxide hydrolase deficiency alters pancreatic islet size and improves glucose homeostasis in a model of insulin resistance. *Proc Natl Acad Sci USA*. 108:9038–9043.
23. Seril DN, Liao J, Ho KL, Warsi A, Yang CS, Yang GY. Dietary iron supplementation enhances DSS-induced colitis and associated colorectal carcinoma development in mice. *Dig Dis Sci*. 2002;47:1266–1278.
24. Seril DN, Liao J, Ho KL, Yang CS, Yang GY. Inhibition of chronic ulcerative colitis-associated colorectal adenocarcinoma development in a murine model by N-acetylcysteine. *Carcinogenesis*. 2002;23:993–1001.
25. Seril DN, Liao J, Lu G, Yang CS, Yang G-Y. Increased susceptibility of ulcerative colitis-associated carcinoma development in Ogg1 knockout mice. *The Proceeding of 96th AACR Annual Meeting,* 2005.
26. Yang J, Schmelzer K, Georgi K, Hammock BD. Quantitative profiling method for oxylipin metabolome by liquid chromatography electrospray ionization tandem mass spectrometry. *Anal Chem*. 2009;81:8085–8093.
27. Deng X, Li H, Tang YW. Cytokine expression in respiratory syncytial virus-infected mice as measured by quantitative reverse-transcriptase PCR. *J Virol Methods*. 2003;107:141–146.
28. Vogel CF, Nishimura N, Sciullo E, Wong P, Li W, Matsumura F. Modulation of the chemokines KC and MCP-1 by 2,3,7,8-

tetrachlorodibenzo-p-dioxin (TCDD) in mice. *Arch Biochem Biophys*. 2007;461:169–175.
29. Kinoshita T, Tomiyama S. Free radicals in inner ear immune responses; immunohistochemical study of myeloperoxidase. *Nippon Jibiinkoka Gakkai Kaiho*. 1994;97:1608–1612.
30. Newman JW, Morisseau C, Harris TR, Hammock BD. The soluble epoxide hydrolase encoded by EPXH2 is a bifunctional enzyme with novel lipid phosphate phosphatase activity. *Proc Natl Acad Sci USA*. 2003;100:1558–1563.
31. Tran KL, Aronov PA, Tanaka H, Newman JW, Hammock BD, Morisseau C. Lipid sulfates and sulfonates are allosteric competitive inhibitors of the N-terminal phosphatase activity of the mammalian soluble epoxide hydrolase. *Biochemistry*. 2005;44: 12179–12187.
32. Enayetallah AE, French RA, Barber M, Grant DF. Cell-specific subcellular localization of soluble epoxide hydrolase in human tissues. *J Histochem Cytochem*. 2006;54:329–335.
33. Gao J, Liao J, Yang GY. CAAX-box protein, prenylation process and carcinogenesis. *Am J Transl Res*. 2009;1:312–325.
34. Bu DX, Griffin G, Lichtman AH. Mechanisms for the anti-inflammatory effects of statins. *Curr Opin Lipidol*.
35. Massonnet B, Normand S, Moschitz R, et al. Pharmacological inhibitors of the mevalonate pathway activate pro-IL-1 processing and IL-1 release by human monocytes. *Eur Cytokine Netw*. 2009;20:112–120.
36. Singh UP, Singh S, Iqbal N, Weaver CT, McGhee JR, Lillard JW Jr. IFN-gamma-inducible chemokines enhance adaptive immunity and colitis. *J Interferon Cytokine Res*. 2003;23:591–600.
37. Khan WI, Motomura Y, Wang H, et al. Critical role of MCP-1 in the pathogenesis of experimental colitis in the context of immune and enterochromaffin cells. *Am J Physiol Gastrointest Liver Physiol*. 2006;291:G803–G811.
38. Morisseau C, Goodrow MH, Newman JW, Wheelock CE, Dowdy DL, Hammock BD. Structural refinement of inhibitors of urea-based soluble epoxide hydrolases. *Biochem Pharmacol*. 2002;63: 1599–1608.
39. Schmelzer KR, Inceoglu B, Kubala L, et al. Enhancement of antinociception by coadministration of nonsteroidal anti-inflammatory drugs and soluble epoxide hydrolase inhibitors. *Proc Natl Acad Sci USA*. 2006;103:13646–13651.
40. Yang J, Schmelzer K, Georgi K, Hammock BD. Quantitative profiling method for oxylipin metabolome by liquid chromatography electrospray ionization tandem mass spectrometry. *Anal Chem*. 2009;81:8085–8093.
41. Kaufmann HJ, Taubin HL. Nonsteroidal anti-inflammatory drugs activate quiescent inflammatory bowel disease. *Ann Intern Med*. 1987;107:513–516.
42. Reuter BK, Asfaha S, Buret A, Sharkey KA, Wallace JL. Exacerbation of inflammation-associated colonic injury in rat through inhibition of cyclooxygenase-2. *J Clin Invest*. 1996;98:2076–2085.
43. Berg DJ, Zhang J, Weinstock JV, et al. Rapid development of colitis in NSAID-treated IL-10-deficient mice. *Gastroenterology*. 2002;123:1527–1542.
44. Planaguma A, Titos E, Lopez-Parra M, et al. Aspirin (ASA) regulates 5-lipoxygenase activity and peroxisome proliferator-activated receptor alpha-mediated CINC-1 release in rat liver cells: novel actions of lipoxin A4 (LXA4) and ASA-triggered 15-epi-LXA4. *Faseb J*. 2002;16:1937–1939.
45. Harizi H, Juzan M, Pitard V, Moreau JF, Gualde N. Cyclooxygenase-2-issued prostaglandin e(2) enhances the production of endogenous IL-10, which down-regulates dendritic cell functions. *J Immunol*. 2002;168:2255–2263.
46. Ham EA, Soderman DD, Zanetti ME, Dougherty HW, McCauley E, Kuehl FA Jr. Inhibition by prostaglandins of leukotriene B4 release from activated neutrophils. *Proc Natl Acad Sci USA*. 1983;80:4349–4353.
47. Flamand N, Surette ME, Picard S, Bourgoin S, Borgeat P. Cyclic AMP-mediated inhibition of 5-lipoxygenase translocation and leukotriene biosynthesis in human neutrophils. *Mol Pharmacol*. 2002;62:250–256.
48. Chou RC, Kim ND, Sadik CD. Lipid-cytokine-chemokine cascade drives neutrophil recruitment in a murine model of inflammatory arthritis. *Immunity*, 33:266–278.